

Frequency-domain photoacoustic phased array probe for biomedical imaging applications

Sergey Telenkov,^{1,*} Rudolf Alwi,¹ Andreas Mandelis,¹ and Arthur Worthington²

¹Center for Advanced Diffusion Wave Technologies, MIE, University of Toronto,
5 King's College Road, Toronto, Ontario M5S 3G8, Canada

²Department of Physics, Ryerson University, 350 Victoria Street, Toronto, Ontario M5B 2K3, Canada

*Corresponding author: sergeyt@mie.utoronto.ca

Received June 3, 2011; revised October 18, 2011; accepted October 18, 2011;
posted October 19, 2011 (Doc. ID 148620); published November 25, 2011

We report the development of a frequency-domain biomedical photoacoustic imaging system that utilizes a continuous-wave laser source with a custom intensity modulation pattern, ultrasonic phased array for signal detection, and processing coupled with a beam-forming algorithm for reconstruction of photoacoustic correlation images. Sensitivity to optical contrast was demonstrated using tissue-mimicking phantoms and *in-vivo* tissue samples. © 2011 Optical Society of America
OCIS codes: 110.5125, 110.7170, 110.3010, 170.3880.

Noninvasive photoacoustic (PA) imaging of tissue vascular network relies on optically induced pressure waves to visualize blood vessel position and oxygen content of blood hemoglobin [1–4]. Combining conventional ultrasound (US) and PA instrumentation in one system makes high-speed PA imaging possible. Real-time systems for imaging of human hand vasculature and cardiovascular dynamics in a small animal have been reported in the literature [5,6]. Additionally, simultaneous coregistration of the two different contrast mechanisms [7] may increase the diagnostic capability of US.

This Letter reports the development of a photoacoustic imaging system that employs an intensity-modulated continuous-wave (CW) laser source for acoustic wave generation and a conventional US phased array probe for signal detection. Detailed descriptions of this technique, also called frequency-domain photothermoacoustics (FD-PTA), operating with a single-element US transducer were given elsewhere [8,9]. The present Letter reports on further developments of the FD-PTA method using a transducer phased array for B-mode imaging of phantoms and blood vessels *in-vivo*. While the use of transducer arrays in general, and phased arrays in particular, is quite common in US and pulsed PA imaging, their application for B-mode imaging with relatively long (≥ 1 ms) optical excitation and very low signal-to-noise ratio (SNR) is unique. Our method of spatially-resolved PA imaging employs millisecond-long optical pulses with the laser intensity modulated according to a specific pattern, while a digital matched filter provides signal compression in a way similar to radar and sonar technologies [10]. As a result, the reconstructed image is the spatial cross-correlation function between the PA response and the reference signal used for laser source modulation. Such correlation processing increases the SNR by several orders of magnitude [11] and preserves the axial resolution at less than 1 mm.

In the PA system shown in Fig. 1, we used a standard ultrasonic 64-element phased array probe (GE Parallel Design, Inc., Phoenix, Arizona) with central frequency 3.5 MHz, 80% mean bandwidth at -6 dB, and pitch 0.254 mm. A simple example of modulation waveforms suitable for efficient pulse compression is a linearly

frequency-swept (chirp) signal. In our system, laser irradiation at 1064 nm emitted by a fiber laser (IPG Photonics, Massachusetts) was continuously modulated by an acousto-optic modulator (Neos Technologies, Florida) driven by chirp waveforms produced by a function generator. The typical duration of the chirps with frequency sweeps in the range 1–5 MHz was 1 ms (repetition rate 1 kHz). Typically 100–1000 chirps were coherently averaged to increase SNR of the incoming signals. The laser beam with diameter about 3 mm and mean power 0.1–1 W was incident on the sample surface through a container with coupling water at an oblique angle ($< 20^\circ$). The coupling water was in contact with the sample surface through a thin transparent plastic film. For the purpose of imaging experiments two types of tissue phantoms were prepared: one was made using PVC-Plastisol [12] with dispersed MgO_2 nanoparticles and the second utilized a water solution of Intralipid suspension with concentration 0.24% by volume. Measurements of the scattering coefficient of the PVC phantom using the Monte Carlo technique gave the reduced scattering coefficient $\mu'_s = 4 \text{ cm}^{-1}$ ($g = 0.9$). To simulate an optical heterogeneity, an inclusion with dimensions $1 \text{ cm} \times 1 \text{ cm} \times 0.5 \text{ cm}$ of the same material stained with black color paint (absorption coefficient 4 cm^{-1} at 1064 nm) was inserted into the PVC phantom at depth $\sim 1.5 \text{ cm}$. The liquid phantom contained two inclusions with $\mu_a = 2$ and 4 cm^{-1} , respectively. The inclusion depth was varied using a micropositioning stage. Parallel data acquisition

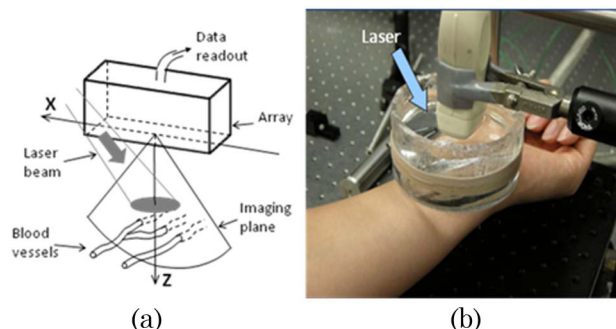


Fig. 1. (Color online) Schematic of frequency-domain PA imager (left) and system setup for *in-vivo* imaging (right).

and signal processing were implemented using modular 8-channel analog-to-digit converters (PXI-5105) and Lab-View software package (National Instruments, Austin, Texas). The current implementation of the PA probe did not allow simultaneous acquisition of all 64 channels with high sampling rate. To expedite data collection, we developed a parallel-sequential algorithm that enables parallel readout of a subarray of eight elements sequentially multiplexed over the entire array using four programmable switch boards (PXI-2593). Although such parallel-sequential data acquisition is slower than a truly parallel scheme, it provides an inexpensive and flexible alternative for readout of multiple channels within acceptable time frames. Moreover, the modular PXI architecture permits easy hardware expansion to increase the total number of channels and the size of the parallel subarray, which is important for utilization of various ultrasonic arrays with the PA probe. Since FD-PTA acquires millisecond-long signals at a multi-MHz sampling rate, the large data arrays necessitate high-speed processing using frequency-domain signal representation and fast Fourier transforms (FFT) for correlation processing. Complete signal processing and image formation in the PA probe is accomplished in three steps. First, signal data are collected from all 64 transducer elements and stored in the computer memory. Second, the complex-valued cross-correlation function $B_i(t)$ of each element is computed using the Fourier transforms of the i th sensor signal $S_i(\omega)$ and the reference modulation waveform $S_r(\omega)$:

$$B_i(t - \tau) = \frac{1}{2\pi} \int_{-\infty}^{+\infty} S_r^*(\omega) S_i(\omega) e^{i\omega(t-\tau)} d\omega. \quad (1)$$

The third stage of signal processing concerns B-mode image reconstruction by forming multiple receiving beams electronically steered over the area of interest. In the standard delay-and-sum beamforming, the beam in the direction given by the angle θ is formed by coherent summation of all sensor signals as

$$u(t, \theta) = \sum_{i=0}^{N-1} w_i \cdot B_i \left(t - \frac{x_i}{c_a} \sin \theta \right), \quad (2)$$

where w_i are apodization or shading coefficients, x_i is the coordinate of the i th sensor, and N is the total number of sensors in a transducer array. For the shading coefficient we used one of the standard window functions. For near-field imaging, the delay time in Eq. (2) also includes a term quadratic with respect to x_i to take into account the wavefront curvature, which is essential for dynamic focusing. As a result of correlation processing and beamforming, a PA correlation image can be displayed as a sector image similar to conventional US. At the present time, signal processing is carried out off-line in postacquisition, which typically requires two minutes to obtain the resulting image.

Three series of imaging measurements were conducted to verify system performance and its capability to detect optical heterogeneities: first, we imaged discrete pointlike optical inclusions in the PVC material to determine spatial resolution of the PA probe; next, we used the light scattering (PVC and Intralipid-based) phantoms to

image position and size of optical inclusions; and finally, imaging of blood vessels *in-vivo* was tested using the wrist of a human volunteer. Initially, the probe point spread function (PSF) was determined using point sources embedded in clear media at different distances from the sensor array. The theoretical PSF shown in Fig. 2(a) was reconstructed using our beamforming algorithm with parameters of the transducer array and the frequency-swept point sources positioned at the depth ranging from 1.5 to 6 cm. Gaussian white noise was added to the input signals to simulate detection with $\text{SNR} = -34$ dB.

Measurements of the PSF were carried out using five cotton threads (0.2 mm in diameter) positioned at different depths and exposed sequentially to the modulated laser source. Results of the measurements are shown in Fig. 2(b) as a mosaic of five sector scans obtained for the PA sources positioned at the depths 2–5.5 cm. The results were consistent with the theoretical beam pattern and gave the axial resolution about 1 mm independent on depth while lateral resolution at the depth of 3.2 cm was about 2.7 mm. Imaging of optical heterogeneities in the light-scattering media with the PA probe and coded optical excitation is shown in Fig. 3. Prior to PA imaging, the PVC phantom was scanned with a conventional US system (Ultrasonix, British Columbia, Canada) to determine the exact position of the inclusion. Since the inclusion was prepared from the same material, acoustic contrast was negligible and the resulting image contrast was very low. The inclusion position was identified as an area with slightly reduced speckle density and shown in Fig. 3(a) by a dashed rectangle. On the other hand, imaging the same phantom with the PA phased array probe [Fig. 3(b)] clearly shows optical contrast due to the increased light absorption in the subsurface chromophore and generation of acoustic waves. The upper spot in Fig. 3(b) is due to the laser beam (mean power ~ 1 W) impinging on the surface, while the bright line at 1.5 cm below the surface indicates the top surface of the inclusion.

Similarly, two discrete chromophores immersed in the Intralipid solution at 1 cm depth were imaged by the PA probe. The resulting correlation image [Fig. 3(c)] reveals their position and lateral dimensions (arrow). The signals observed below the two main peaks correspond to acoustic reflections from the inclusion back surface. For the human wrist image in Fig. 3(d), the incident laser beam was maintained at the safety level [13] during data

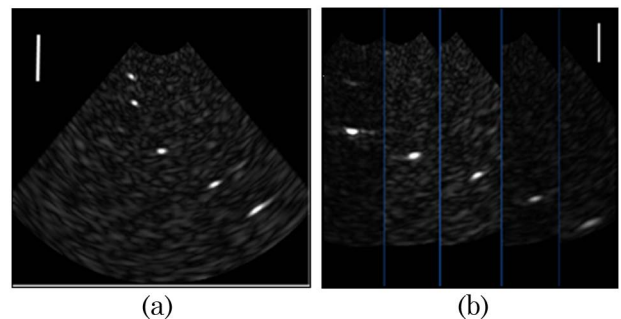


Fig. 2. (Color online) System PSF computed using array parameters and simulated point sources (a) and measured using cotton threads imbedded in a PVC phantom (b). The vertical scale bar is 1 cm long.

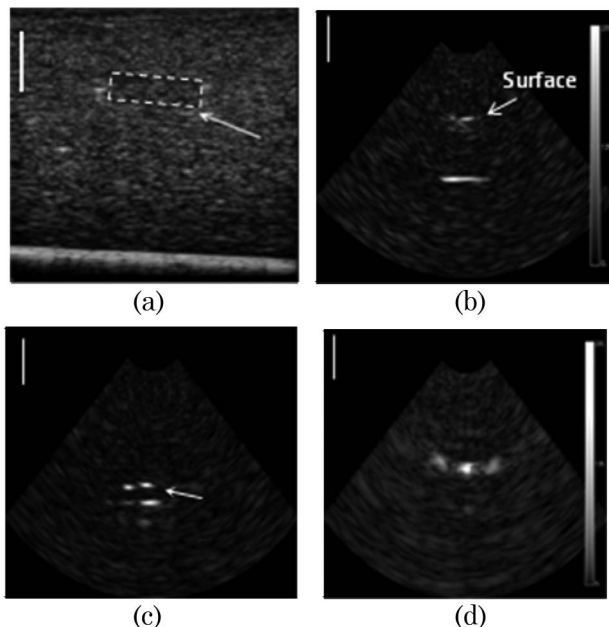


Fig. 3. Ultrasound image (a) and PA probe image (b) of the PVC phantom with a subsurface inclusion. Image of discrete chromophores (c) immersed in Intralipid solution and blood vessels in a human wrist (d). The vertical scale bar is 1 cm long.

acquisition. The reconstructed sector image shows discrete bright spots related to sound generation in the near-surface blood vessels of the wrist.

In conclusion, we reported the development of a FD-PTA system utilizing a US phased array probe and intensity-modulated optical excitation with specific chirp coding to improve SNR. We have demonstrated that the FD-PTA methodology coupled with a multielement sensor array can deliver B-mode spatially-resolved correlation images of PA sources in tissuelike scattering media. The described phased array PA probe may be used for various biomedical applications such as noninvasive imaging of human vasculature and imaging of optical

contrast related to tissue abnormalities. Since our system employs a standard probe and typical image reconstruction algorithm, it can be conveniently integrated into clinical US instrumentation for high-speed and interleaved image coregistration of tissues.

This work was supported by Natural Sciences and Engineering Research Council (NSERC) through Discovery and Strategic grants and by the Premier's Discovery Award, Ministry of Research and Innovation, Ontario. We thank Drs. M. Kolios and B. Soroushian for assistance with US image acquisition and Monte Carlo measurements. Ultrasonix Inc. contribution of an US phased array probe to this project is gratefully acknowledged.

References

1. A. Roggan, M. Friebel, K. Dorschel, A. Hahn, and G. Muller, *J. Biomed. Opt.* **4**, 36 (1999).
2. R. G. M. Kolkman, M. J. Mulder, C. P. Glade, W. Steenbergen, and T. G. Van Leeuwen, *Lasers Surg. Med.* **40**, 178 (2008).
3. H. F. Zhang, K. Maslov, G. Stoica, and L. V. Wang, *Nat. Biotechnol.* **24**, 848 (2006).
4. S. A. Ermilov, T. Khamapirad, A. Conjusteau, M. Leonard, R. Lacewell, K. Mehta, T. Miller, and A. Oraevsky, *J. Biomed. Opt.* **14**, 024007-1 (2009).
5. R. G. M. Kolkman, P. J. Brands, W. Steenbergen, and T. G. van Leeuwen, *J. Biomed. Opt.* **13**, 050510-1 (2008).
6. R. J. Zemp, L. Song, R. Bitton, K. K. Shung, and L. V. Wang, *Opt. Express* **16**, 18551 (2008).
7. A. Aguirre, P. Guo, J. Gamelin, S. Yan, M. Sanders, M. Brewer, and Q. Zu, *J. Biomed. Opt.* **14**, 054014-1 (2009).
8. S. Telenkov and A. Mandelis, *J. Appl. Phys.* **105**, 102029-1 (2009).
9. S. Telenkov and A. Mandelis, *J. Biomed. Opt.* **14**, 044025-1 (2009).
10. C. E. Cook and M. Bernfeld, *Radar Signals. An Introduction to Theory and Application* (Academic, 1967).
11. S. Telenkov and A. Mandelis, *Rev. Sci. Instrum.* **81**, 124901-1 (2010).
12. G. Spirou, A. Oraevsky, I. A. Vitkin, and W. Whealan, *Phys. Med. Biol.* **50**, N141 (2005).
13. American National Standard, ANSI Z136.1-2007 77.